Chapter 11
Reaction–Diffusion Controllers for Robots

Andrew Adamatzky, Benjamin De Lacy Costello, and Hiroshi Yokoi

11.1 Introduction

Excitable systems, particularly spatially extended media, exhibit a wide variety of travelling patterns and different modes of interaction. The Belousov–Zhabotinsky [1] (BZ) reaction is the most well known and extensively studied example of non-linear chemical system exhibiting complex behaviour. The BZ reaction is well known to exhibit spontaneous oscillatory behaviour. The mechanistic details are complex but involve a fine balance between an auto-catalytic oxidation process and an inhibitor of the autocatalytic reaction. If the chemical conditions are altered beyond the point where the reaction exhibits spontaneous oscillatory behaviour, then the BZ reaction exhibits a property known as excitability. An excitable system has a steady state and is stable to small perturbations; however, if the perturbations exceed a critical threshold, then the system responds with an excitation event. In the case of a thin layer architecture, this results in a circular wave travelling from the source of the perturbation. Parts of the wave front annihilate when they reach the boundaries or collide with other fronts; however, other parts will propagate across the whole free area of the reactor. Because the BZ system is excitable and due to the properties of wave propagation, it can be considered as a uniform locally connected primitive neural network (a type of neural network similar to that in *Protozoa*). The information processing capabilities of BZ media are relatively well studied in the framework of reaction–diffusion computing [2, 3]. A reaction–diffusion processor is the term used to describe an experimental chemical reactor which computes by sensibly, purposefully and predictably transforming the initial local disturbances in the chemical concentration profiles – the data pattern – into dynamical structures such as travelling excitation waves, or stationary output such as a spatial distribution of precipitate – result patterns – in these processors the computation is implemented via the interaction of either diffusive or phase waves in the chemical system [2, 3]. Reaction–diffusion processors of this general type possess an amorphous structure (absence of any type of rigid hardware-like architecture in the processor's liquid

A. Adamatzky and M. Komosinski (eds.), *Artificial Life Models in Hardware*,

© Springer-Verlag London Limited 2009

phase) and massive parallelism (a thin layer Petri dish may contain thousands of elementary computing micro-volumes).

The field of reaction–diffusion chemical computing is rapidly expanding and features a number of experimental prototypes capable of solving a wide range of problems: computational geometry, image processing, implementation of logical gates and constructing simple memory devices; see detailed overview in [2, 3]. Some of the unique and desireable features of reaction–diffusion computers [2, 3] include (1) massive-parallelism – each micro-volume of the liquid-phase chemical system acts as an elementary processor and there are potentially many thousands of micro-volumes in a centimetre cubed domain of the medium; (2) local connectivity – the chemical medium's micro-volumes automatically update their states (local concentrations of chemical species) depending on the combined state of their immediate neighbours; (3) potentially massive-parallel input and outputs – data are represented by distributed concentration profiles or gradations of the medium's illumination, while results are configurations of precipitate concentration or dissipative excitation patterns that may be recorded optically; (4) self-healing and self-reconfiguration due to the liquid-phase or gel-based structure of the computing substrate and the fact that elementary processing units are identical; (5) dynamically reprogrammable architectures – computation is implemented by travelling waves or wave-fragments and therefore, this site of the medium acts as a momentary wire. However, annihilation of excitation waves occurs enabling input of additional data streams with time. These characteristics of chemical systems make them ideally tailored for the implementation of novel and emerging architectures of robotic controllers and embedded processors for smart structures and actuators.

In the first part of the chapter, we show that chemical reaction–diffusion processors based on the BZ medium as specified in Sect. 11.2, can be successfully used as robot controllers in various experimental setups and applications.

We start our journey by describing approaches to mounting a chemical computer onboard of a mobile robot. This allows for dynamical interaction between the robot, its environment and the chemical computer. In Sect. 11.3, we define the problem of controlling robot navigation with chemical controllers and outline a possible solution, where we describe a mobile robot with an on-board chemical controller, and discuss how we can use the chemical controller to guide the robot.

In further work, we make the transition from guided/manipulated robots to robots capable of manipulating several objects at once. In Sect. 11.4, we couple a simulated abstract parallel manipulator with an experimental BZ chemical medium, whereby, the excitation dynamics in the chemical system are reflected by changing the OFF–ON mode of elementary actuating units. We convert experimental snapshots of the spatially distributed chemical system to a force vector field and then simulate the motion of manipulated objects in the force field, thus, achieving reaction–diffusion media controlled actuation.

The controllers described in Sects. 11.3 and 11.4 are used predominantly in an open-loop device mode, where the robot or robot manipulator is controlled by the chemical medium but does not provide any useful explicit (only implicit, via human operator) feedback to the chemical media controlling it. We specify this as useful

because in robot, taxis movement of the robot provides physical disruption of the chemical processor, but the results are yet difficult to translate to sensible feedback. Until our recent paper [4], there were no experimental results concerning the real-time interaction of robotic devices with chemical reaction–diffusion controllers. In that paper, we designed and implemented a series of experiments concerning the two-way interactions between a spatially distributed excitable chemical controller and a robotic hand. The interactions are two-way because the waves travelling in the chemical media control the movement of the fingers and then the fingers physically (disturb the solution) and chemically (disperse activator from small pipettes placed on the fingers) interact with the reaction–diffusion controller. In Sect. 11.5 we present an overview of our results, see details in [4].

Some people may consider that coupling gel or liquid phase chemical processors with rigid silicon hardware and robotic devices are a bit eccentric and predominantly a curiosity-driven activity. They are of course partly right as conventional hardware is not the right application domain for chemical processors or reaction–diffusion processors in general. In fact reaction–diffusion processors would be better employed in amorphous spatially extended, distributed and reconfigurable architectures with distributed sensor and effector arrays. Such architectures are not yet available in a complete form and therefore, to demonstrate the feasibility and future potential of the reaction diffusion based approach, we employed a living analogue of a reaction–diffusion system encapsulated in a functional elastic membrane – plasmodium of *Physarum polycephalum*. The large size of the plasmodium allows the single cell to be highly amorphous. The plasmodium exhibits synchronous oscillation of cytoplasm throughout its cell body, and oscillatory patterns control the behaviour of the cell. The oscillatory cytoplasm of the plasmodium can be seen as a spatially extended excitable reaction–diffusion based medium.

In the Plasmodium, all the parts of the cell behave cooperatively in exploring the domain space, searching for nutrients via an optimized network of streaming protoplasm. Due to its unique features and ease of experimentation, the plasmodium became a test biological substrate for implementation of various computational tasks. The fact that it is encapsulated in an elastic membrane means that plasmodium are not only capable of computing spatially distributed data-sets but also the physical manipulation of elements of the data-sets. If a sensible, controllable and, ideally, programmable movement of the plasmodium could be achieved, this would open the way for experimental implementations of amorphous robotic devices.

In this chapter, we discuss a set of scoping experiments that aim to establish links between Physarum based computing and Physarum robotics. For the purpose of the experiments, we have chosen the surface of water as a physical substrate for the plasmodiums development to study how the topology of the plasmodium network can be dynamically updated, without the requirement for the plasmodium to be stuck to a non-liquid substrate. With this sytem we have studied the possibility of manipulating small objects floating on the surface with the plasmodium's pseudopodia. In Sect. 11.6, we show that the plasmodium of Physarum is capable of computing basic spanning trees and also of manipulating lightweight objects.

11.2 BZ Medium

A thin layer BZ medium can be prepared using a recipe adapted from [5]: an acidic bromate stock solution incorporating potassium bromate and sulphuric acid ($[BrO_3^-] = 0.5\,M$ and $[H^+] = 0.59\,M$) (Solution A); solution of malonic acid (solution B) ($[CH_2(CO_2H)_2] = 0.5\,M$), and sodium bromide (solution C) ($[Br^-] = 0.97\,M$). Ferroin (1,10-phenanthroline iron-II sulphate, 0.025 M) is used as a catalyst and a visual indicator of the excitation activity in the BZ medium. To prepare a thin layer of the BZ medium, we mix solutions A (7 ml), B (3.5 ml), C (1.2 ml) and finally when the solution becomes colourless ferroin (1 ml) is added and the mixture is transferred to a Petri dish (layer thickness 1 mm). Excitation waves in the BZ reaction can be initiated using a silver colloid solution. This excitable chemical processor is used both on-board the mobile robot and in experiments to control a robotic hand. The processor used to control the actuator array was based on a silica gel sheet of 0.2 mm thickness which had been soaked in 0.01 M ferroin solution for 30 min. The catalyst loaded gel sheet was then placed in a petri dish containing 10 ml of BZ stock solution devoid of the catalyst (see recipe above).

11.3 Robot Taxis

The BZ reaction can be used to assist the navigation of a mobile robot in a real-life environment [6]. Given an on-board thin-layer chemical reactor containing the liquid-phase BZ medium, the chemical medium can be intermittently stimulated to sensibly guide the robot.

To make a BZ controller capable of robot taxis, we prepared a thin layer BZ reaction using a recipe adapted from [5] and detailed in Sect. 11.2. Excitation waves in the BZ reaction are initiated using a silver colloid solution, which is added to the medium via a micro pipette by a human-operator. The chemical controller is placed onboard a wheeled mobile robot (Fig. 11.1a). The robot is about 23 cm in diameter and able to turn on the spot; wheel motors are controlled by Motorola 68332 on-board processor. The robot features a horizontal platform, where the Petri dish (9 cm in diameter) is fixed, and a stand with a digital camera Logitech QuickCam (in 120×160 pixels resolution mode), to record the excitation dynamics. The robot controller and camera are connected to a PC via serial port RS-232 and USB 1.0, respectively.

Because vibrations adversely affect the excitation waves in the BZ system, we endeavoured to make the movements of the robot as smooth as possible. Thus, in our experiments, the robot moves only with a speed of circa $1\,cm\,s^{-1}$. We found that rotational movements were particularly disruptive and caused spreading of the excitation waves from the site of the existing wave fronts faster than would be observed if the process was just diffusion driven. Therefore, to minimize this effect we made the robot rotate with a very low speed of around $1\,deg\,s^{-1}$. The vibrations and rotational movements are only considered adverse for the purpose of the original

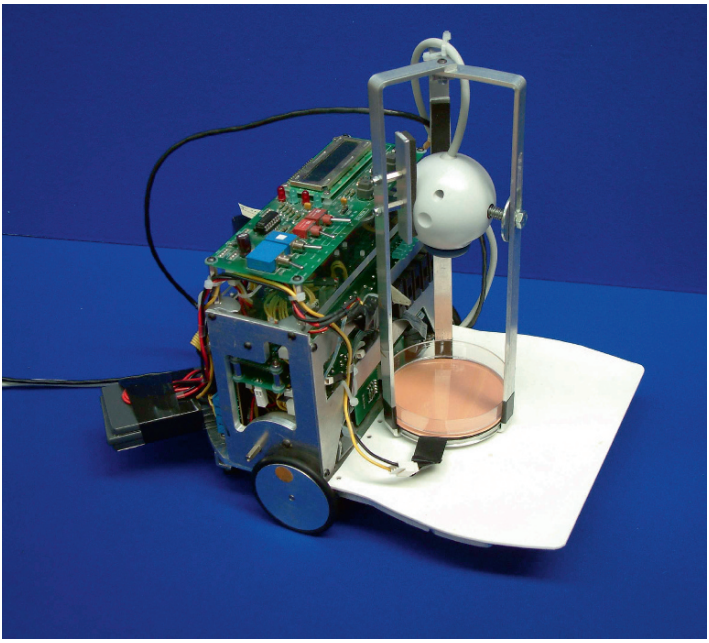

(**a**)

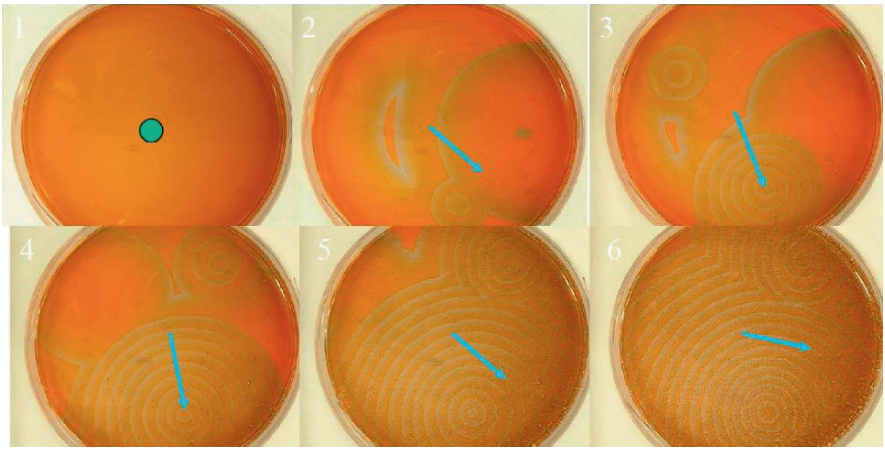

(**b**)

Fig. 11.1 Wheeled robot controlled by BZ medium (**a**) and snapshots of excitation dynamics with the robot's velocity vector extracted (**b**). From [6]

experiments, where we want to establish methods for extracting vectors from the excitation dynamics. In future incarnations, these movements could be used to measure said motion and feedback information to the robot including information about the environment. For example, if the robot collided with an obstacle the physical jolt may be sufficient to reset the excitation dynamics of the chemical controller.

To enhance the images of the excitation dynamics, the Petri dish is illuminated from underneath by a flexible electro-luminescent sheet (0.7 mm thick) cut to the shape of the dish. The sheet, powered through an inverter from the robot's batteries, produces a cool uniform blue light not affecting (at least in conditions of our experimental set-up) physico- chemical processes in the reactor. We found it was preferable to implement experiments in low light to avoid the interference of daylight and lamps.

When the medium was initiated with silver, a local generator of excitation waves is formed (Fig. 11.1b), depending on the amount of activator deployed trains of circular waves (target waves) may evolve. The robot is able to extract the position of the stimulation point, relative to the centre of the chemical reactor by using the topology of the excitation waves. The robot adjusts its velocity vector to match the vector towards the source of stimulation. To guide the robot more precisely, one can excite the chemical medium at several points (Fig. 11.1b). The forced stimulation was simply to test algorithms on board with real chemical controllers and to learn about problems with coupling chemical reactors and robots. Something which was identified as a problem – i.e. physical disruption of chemical waves could actually turn out to be advantageous as it may feed back both direction, velocity and even rotational movement of robot. It should be noted that eventually it was intended for environmental interaction to become the source of stimulation for excitation waves. For example, there are light sensitive analogues of the reaction and information about the robots environment may able to be mapped onto a light sensitive chemical processor and feed information to the robot. It may also be possible to deploy bulk oscillating micro-reactors, which are placed around the robot and are directly electrically coupled to the robots drive motors. The oscillations would be controlled by light levels and if all reactors were coupled, it may be possible to obtain complex information about the robots environment.

The main goal of our research concerning chemical controllers for robots [6] was to develop a stand-alone onboard controller, which could sense and process information from the robot's environment, calculate the current mode of the robots movement and communicate a set of appropriate commands to the robots motor controllers [2, 6].

Therefore, we put the following constraints on a possible solution of the problem. Firstly, an algorithmic solution must be local – if the BZ medium is mapped onto a two-dimensional array, e.g. a cellular automation, then every cell of the array must be able to calculate its own local vector from the configurations of its r-order neighbourhood. Secondly, only spatial data are allowed – a vector towards the position of the stimulation source must be extracted from just one snapshot of the medium's excitation dynamics. In addition, the robot control unit (including sub-systems based in the interfaced PC) is not allowed to remember local or global vectors calculated at previous stages (therefore, we tried to reduce the role of the hardware to interfacing and decoding).

To prove that a vector towards a source of stimulation can be extracted under these three constraints, it is sufficient to demonstrate that the asymmetry of excitation waves is detected from digital snapshots of the medium dynamics.

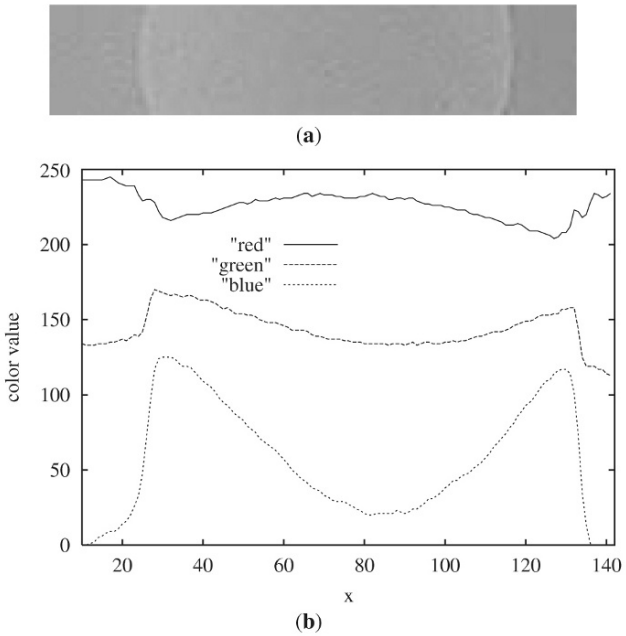

Fig. 11.2 Demonstration of the asymmetry of wave fronts as detected from snapshots of the BZ medium: (**a**) fragment of a snapshot of an expanding target wave; (**b**) values of *red*, *green* and *blue* components of pixels along *x*-axis cross-section averaged along *y*-axis. The distribution preserves its form but exact values in each experiment vary depending on the concentrations of reactants. From [6]

As seen in Fig. 11.2, the shape of the excitation wave front is visually represented by a spatial distribution of red, green and blue components of each pixel's value. The distribution of the blue component efficiently characterizes all parts of the wave front, including the zones corresponding to the sharp excitation event and the zone where the medium gradually returns back to the reduced steady state (excitable state) via the refactory state. Therefore, only the blue component of the pixel colours was necessary to reconstruct the stimulation position. All normals to the wave front, calculated from gradients of the blue colour values, are oriented towards a site where the wave originated. Therefore, a simple analysis of the spatial distribution of normals would give the robot an indicative position of the stimulation source.

The algorithm does not work if the source of stimulation is represented by an almost perfect circular wave front, all parts of which are inside the processed zone of the reactor – in this case all local vectors will cancel each other. However, this can be coped with by introducing a breathing receptive field, which changes its size during experiments, or simply by waiting until some parts of the wave front reach the edges of the reactor and disappear. The dynamically changing receptive field could also reduce the influence of phase waves spontaneously generated at the edges of the reactor.

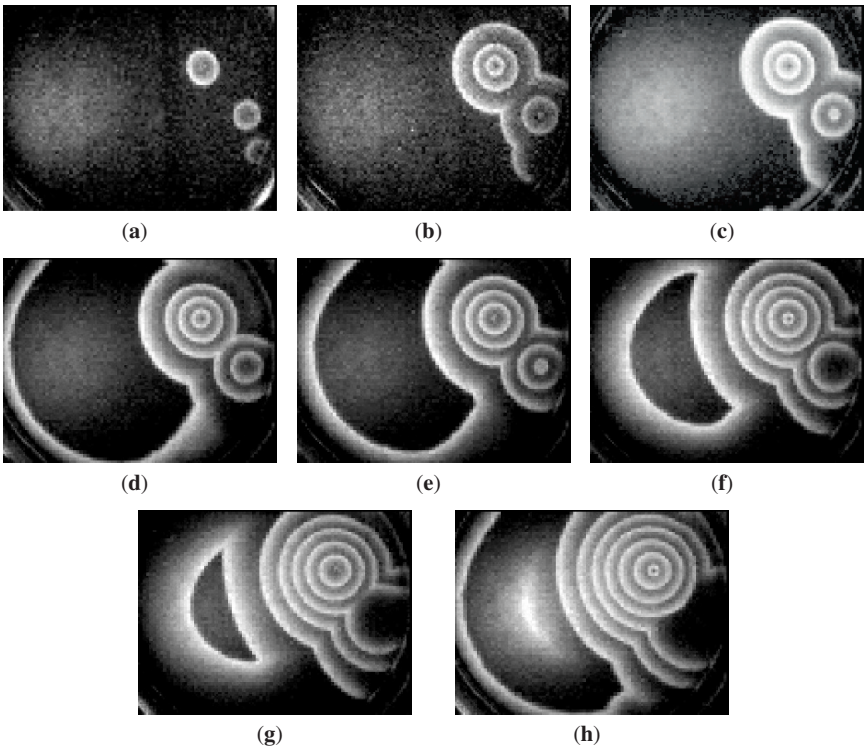

Fig. 11.3 Snapshots of the BZ medium, the intensity of the *blue component* of the pixel colour is displayed. From [6]

Consider the example of global vector extraction from the reactors excitation dynamics in Figs. 11.3 and 11.4. Three sources of target waves were initiated at different time intervals. At first, the robot detects no stimulation because the wavefronts are perfectly closed and circular (Figs. 11.3a and 11.4a). Then the outer wavefront of one of the target waves reaches the edge of the reactor and annihilates by becoming disconnected. The robots control algorithm calculates a vector towards this specific point of stimulation (Figs. 11.3b and 11.4b). At the same time, another wavefront from a secondary source of stimulation also becomes disconnected (in Fig. 11.3a, c–e) causing a deviation in the global vector (Fig. 11.4c–e). The second source of target waves was initiated using a smaller quantity of silver colloid and therefore, only four waves are initiated from the original point of stimulation before the site returns to the steady reduced state. the result is that the global vector rotates back toward the first source of stimulation (Fig. 11.3f–h).

In real life situations, robots are often required to choose between several sources of stimulation. How could this type of decision-making be implemented in an on-board chemical controller? Given two sources of point-wise stimulation, the robot

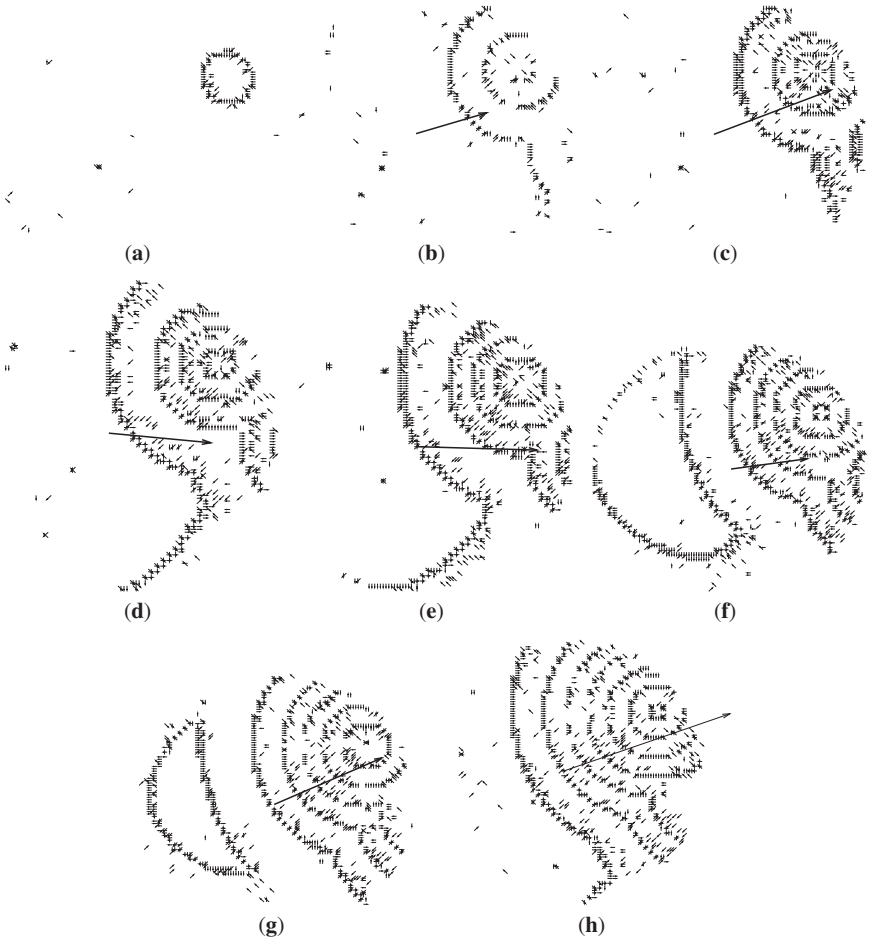

Fig. 11.4 Local vector fields and global vectors (*shown in bold*) extracted from snapshots of BZ medium in Fig. 11.3. From [6]

usually chooses the older source. This is because, as discussed, the oldest stimulation point is represented by predominantly broken wavefronts that have a greater degree of spatial asymmetry and usually a greater number of wave fronts when compared to the more recent sources of stimulation (Fig. 11.5a, b). However, when the older source of excitation disappears or if the newer target wave has a higher frequency of wave initiation, then this will be selected as the current orientation target. Therefore, it can be said that the onboard chemical controller is capable of memorizing the temporal order of the stimulations. Moreover, a fine balance could be achieved between the intensity and time tag of multiple stimulations to achieve a more precise trajectory for the robot's motion.

Once stimulated, the robot moves in circles because it recalculates the position of the stimulation source every time regardless of its previous position and does not remember previously extracted vectors. This circular motion has been described previously in simulation experiments [2] and is a typical behavioural mode for mobile excitable lattices with a wide interval of node sensitivity. Relatively straightforward motion could be achieved by stimulating the chemical reactor twice and positioning these points of stimulation at opposite sites of the reactor, so that a bisector of these two points gives the orientation of the velocity vector. Also the circular motion of a robot can be prevented by increasing the bromide ion concentration and thus, making it impossible for a generator of target waves to persist in the reactor. In this case, just a few wave fronts will travel across the reactor and disappear. Obviously in this case, the robot must analyse snapshots of the medium after longer delays, e.g. once per 10–15 min. To slow down or stop the robot we could 'block' the velocity vector with several sources of wave generation, as shown in Fig. 11.6.

11.4 Open-Loop Parallel Actuators

How can a reaction–diffusion medium manipulate objects? To find out, we coupled a simulated abstract parallel manipulator [7] with an experimental BZ chemical medium. The simulated manipulator is a two-dimensional array of actuating units, each unit can apply a force vector of unit length to the manipulated objects. The velocity vector of the object is derived via the integration of results of all local force vectors acting on the manipulated object.

To demonstrate the potential of the BZ system for manipulating simple objects, we built an interface between the recordings of space-time snapshots of the excitation dynamics and simulated physical objects. At first we calculated the force fields generated by the mobile excitation patterns and then tested the behaviour of an object in these force fields.

This coupling of an excitable chemical medium with a manipulator allows the conversion of experimental data relating to wave movement in the BZ medium into a force vector field and subsequently assess the imparted motion of objects in the changing field, thereby, achieving reaction–diffusion medium controlled actuation [8].

The chemical processor used to perform actuation was prepared following the recipe in Sect. 11.2, see also [5], based on a ferroin catalyzed BZ reaction. A silica gel plate is cut and soaked in a ferroin solution. The gel sheet is placed in a Petri dish and BZ solution added. The dynamics of the chemical system are recorded at 30 s intervals using a digital camera.

The cross-section of the BZ wavefront recorded on a digital snapshot shows a steep rise of red colour values in the pixels at the wavefront's head and a gradual descent in the pixels spanning the wavefront's tail. Assuming that excitation waves push the object, local force vectors generated at each site – a pixel of the digitized image – of the medium should be oriented along the local gradients of the red colour

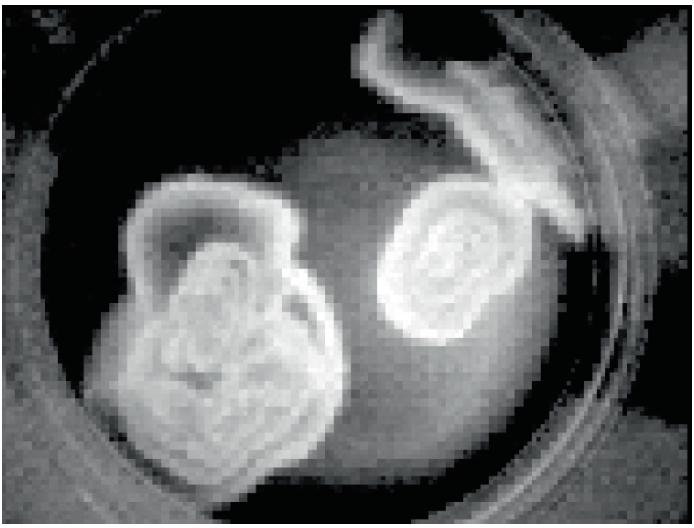

(**a**)

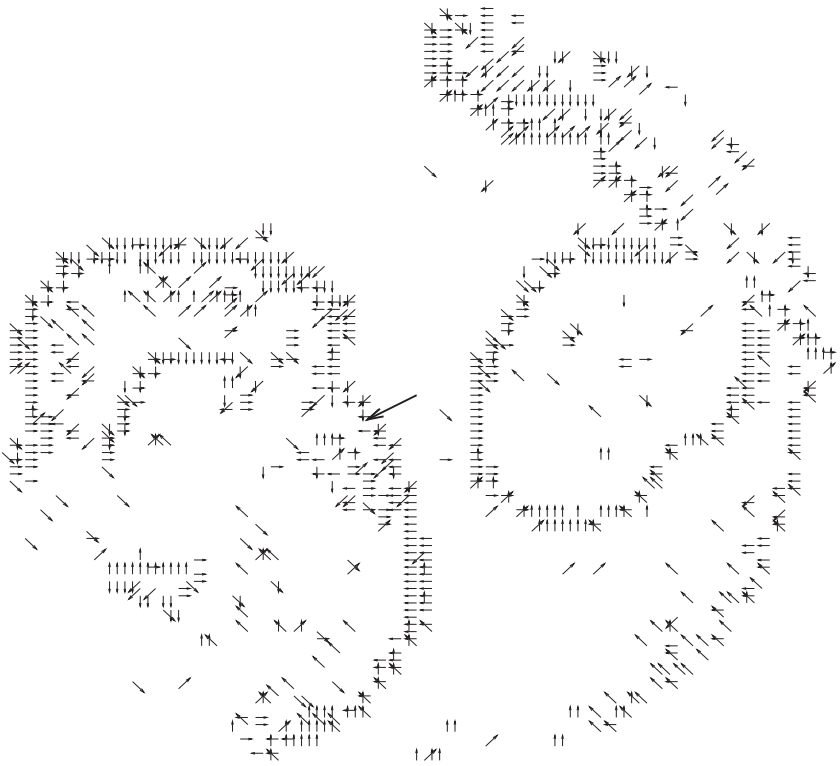

(**b**)

Fig. 11.5 An example of the decision making procedure in a chemical processor: selection of the strongest generator of target waves, representing a "strongest" source of stimulation. (**a**) the blue component of an image of the BZ reaction, (**b**) local vector field and global vector (*in bold*). From [6]

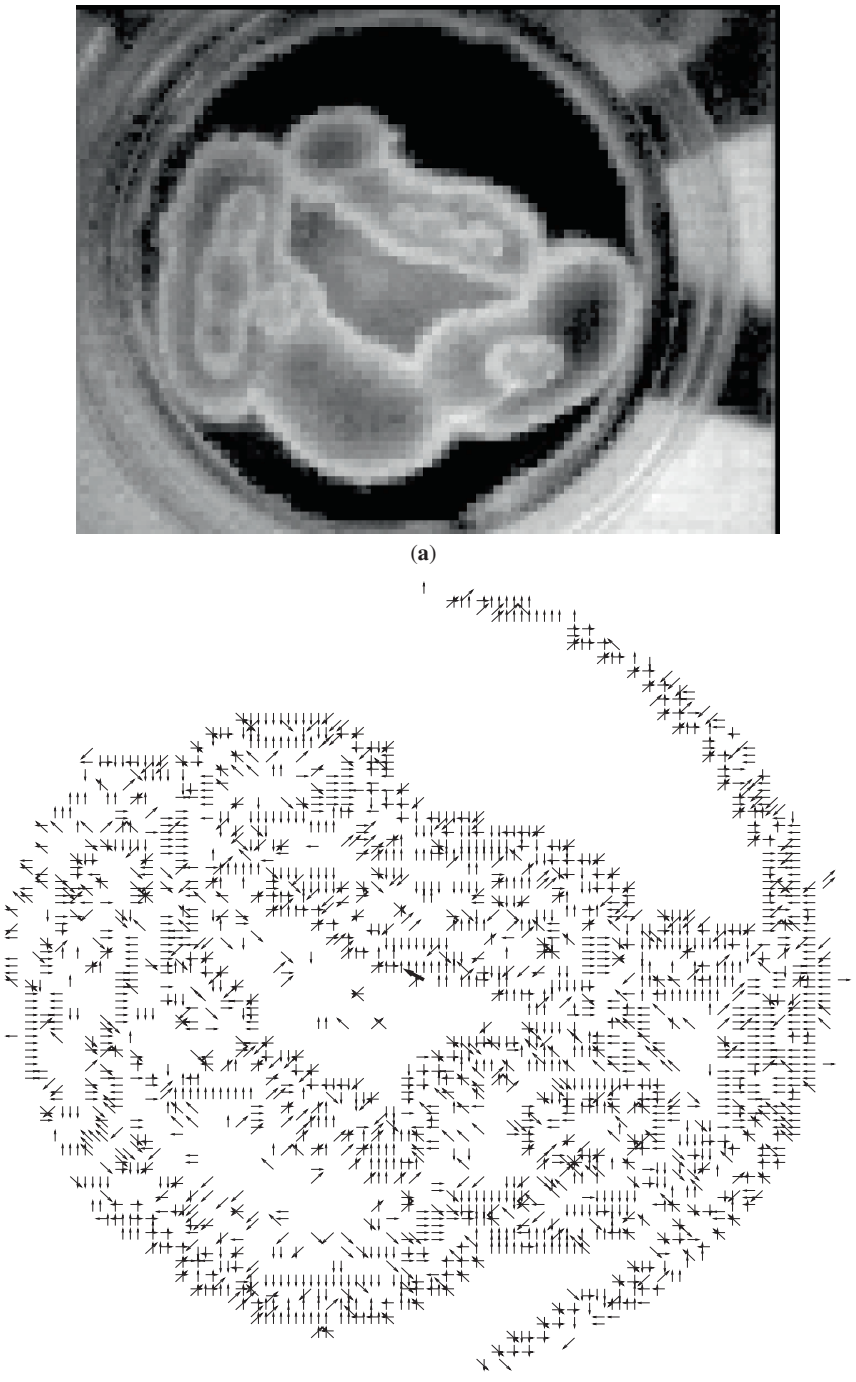

(**a**)

(**b**)

Fig. 11.6 Stopping the robot by "trapping" the global vector between several generators of target waves. (**a**) blue component of BZ image, (**b**) local vector field and global vector (*in bold*). From [6]

values. From the digitized snapshot of the BZ medium, we extract an array based on the red component of the images and then calculate the projection of a virtual vector force at the pixel. An example of force vector field extracted from a fragment of an excitation wavefront is shown in Fig. 11.7.

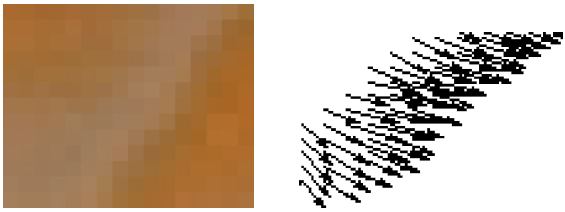

Fig. 11.7 A fragment of an excitation wavefront in the BZ medium (**a**) local force vectors extracted (**b**). From [7]

Force fields generated by the excitation patterns in a BZ system (Fig. 11.8) result in tangential forces being applied to a manipulated object, thus, causing translational and rotational motion of the object [7].

When placed on the simulated manipulating surface, pixel-objects move at random in the resting domains of the medium; however, via random drift each pixel-object does eventually encounter a domain of co-aligned vectors – representing the excitation wave front of the BZ medium – and is therefore, translated along the vectors. An example of several pixel-objects transported on a "frozen" snapshot of the chemical medium is shown in Fig. 11.9.

Rough trajectories of pixel-objects (Fig. 11.9a) show distinctive intermittent modes of random motion separated by modes of directed 'jumps' guided by travelling wave fronts; compare Fig. 11.9a, c. Smoothed trajectories of pixel-objects (Fig. 11.9b) show that despite a strong chaotic component in manipulation, pixel-objects are successfully transported to the sites in the medium where two or more excitation wavefronts meet.

The phenomenon of the manipulation of pixel-objects by dynamically changing patterns of excitation reflects, in principle, that of the stationary configurations (Fig. 11.10). At the initial stage, involving excitation target waves originating from several sources of stimulation, but do not fill the entire manipulation space (see e.g. Fig. 11.10, $t = 0$ min and $t = 1$ min) and therefore, the pixel-objects are transported to the resting parts of the medium, where they either continue drifting at random, or they can follow artefact gradations of colour imposed by the external illumination (see trajectories of two pixel-objects, which started their journeys at the right part of the medium's snapshot. Fig. 11.10, $t = 0$ min). Eventually, they are pushed over the domains corresponding to the bisectors' separating parts of the medium relating to the sources of target waves.

The overall speed of pixel-object transportation and in some cases, even success depended on the frequency of wave generation by the various target waves. As a

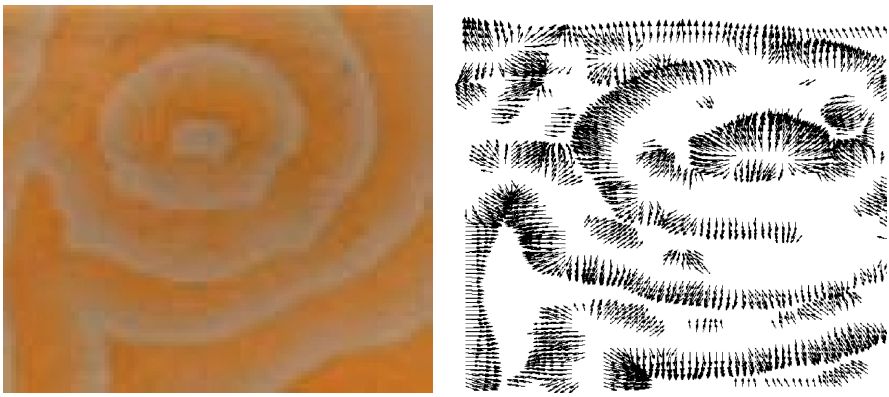

(**a**) (**b**)

Fig. 11.8 Force vector field (**b**) calculated from BZ medium's image (**a**). From [7]

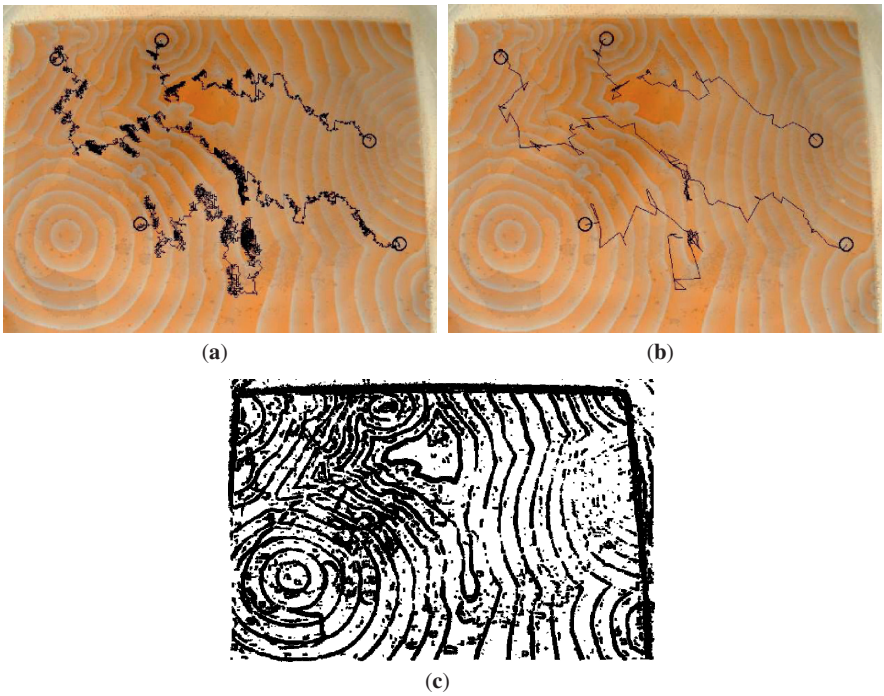

(**a**) (**b**)

(**c**)

Fig. 11.9 Examples of manipulating five pixel-objects using the BZ medium: (**a**) trajectories of pixel-objects, (**b**) jump-trajectories of pixel-objects recorded every 100th time step, (**c**) force vector field, extracted from the BZ snapshot (**a**), used for manipulating pixel-objects. Initial positions of the pixel-objects in (**a**) and (**b**) are shown by *circles*. Note locally noisy drifting of the pixels. From [7]

rule, the higher the frequency the faster the objects are transported. This is because in parts of the medium spanned by low frequency target waves, there are lengthy domains of the reactor, which is in the resting state, resulting in the absence of force vectors. Therefore, pixel-sized object can wander randomly for a long time before encountering the next wave front (compare the pixel-object transported by low-frequency target waves on the right side of Fig. 11.11a with the pixel-object trajectory on the right side of Fig. 11.11a).

Our method of manipulating pixel-objects also works in the conditions of a 'non-ideal' excitable chemical medium. Thus, in the situation when numerous spiral waves emerge in the system (Fig. 11.11b), the pixel-objects bounce off the spirals; an overall southward drift of the objects in Fig. 11.11b is caused by the tendency of excitation wavefronts to be less fragmented in this direction.

Even when the BZ medium resides in a sub-excitable regime (where sources of excitation cause formation of non-target or spiral waves but mostly soliton-like travelling wave-fragments), the pixel-objects can still be sensibly manipulated (see Fig. 11.11c). The objects are pushed by travelling wave-fragments, however, (as shown in Fig. 11.11c) they can very often slip away.

In general, spatially extended objects repeat the overall pattern of motion observed for the pixel-sized objects; however, due to the integration of many force vectors, the motion of planar objects is smoother and less sensitive to the orientation of any particular force-vector.

In experiments, we found that manipulation results depend on the size of the object, thus for example, see Fig. 11.12, a small square shape (starting its journey at the north–west corner of the chemical reactor, Fig. 11.12a) is accelerated by force-vectors, caused by the excitation waves, and passes the central part of the reactor barely changing its trajectory due to collisions with opposing wavefronts. With increasing size of the object, we take account of larger numbers of local vector-forces, and thus, the objects' trajectory becomes more controllable and in Fig. 11.12b we see that the object is sensibly transported to the 'sink' of the force-field, and stays there "indefinitely".

The response of the object to the excitation wave depends also on the wavelength, the shorter the wavelength the larger the acceleration of the object. Thus in Fig. 11.13, the object starts to travel at the "slope" of the target wave before being "bounced" several times between the oncoming wavefronts, then missing the "sink" of the reactor and travelling through the central part of the reactor between the target waves.

By choosing the positions of the initial stimulation of the excitable chemical controller and the initial position of the manipulated object, we can precisely control the trajectory of the manipulated object. Thus in Fig. 11.14, we demonstrate reflection of the triangular shape by the central part of the target wave (Fig. 11.14a) and also by proximal wavefronts of the generator (Fig. 11.14b).

In [7], we also showed that BZ media exhibiting large populations of spiral wave generators exhibit great potential for the directed transportation of the planar shapes. All objects are usually pushed away, toward the periphery of the spiral wave population; however, they can be easily deviated by carefully positioning sources of target

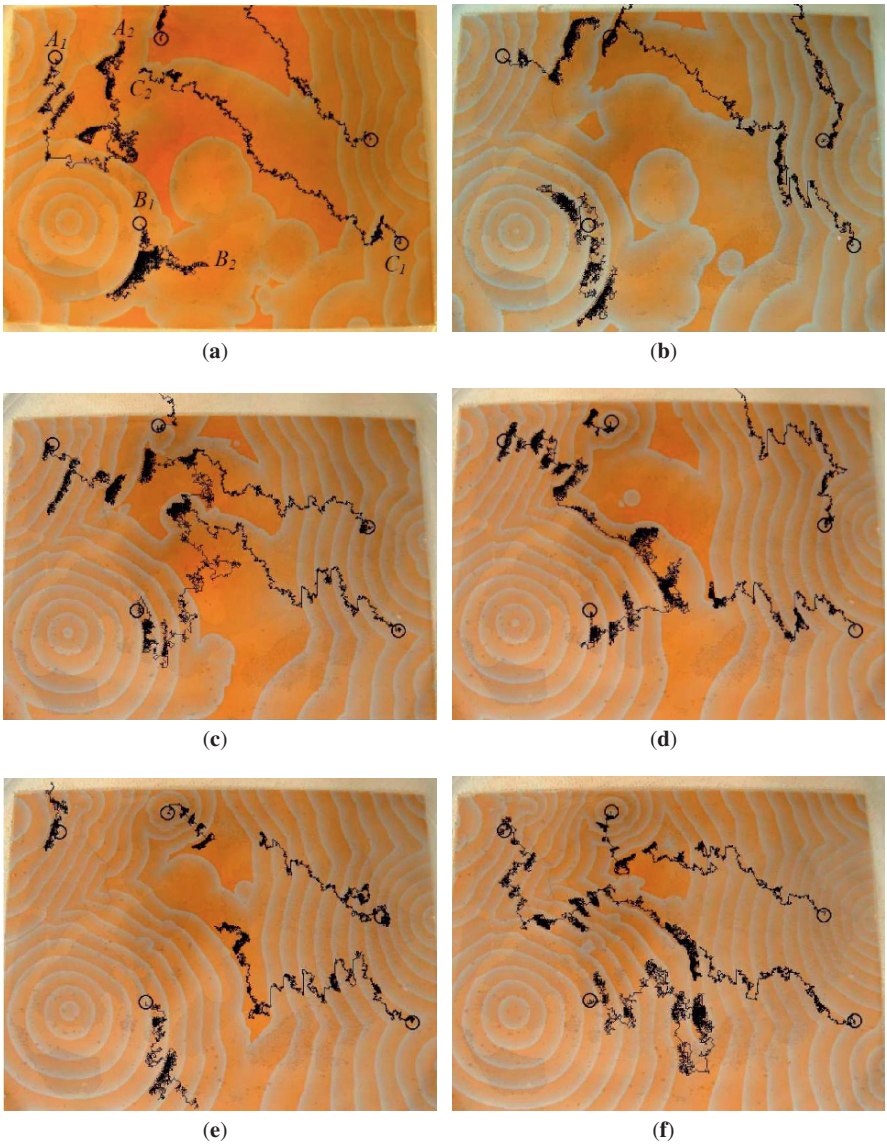

Fig. 11.10 Pixel-objects manipulated by dynamically changing configurations of excitation in the BZ medium. For every snapshot of the medium pixel-objects are transported from the same original points for 10,000 steps of discrete time. Initial positions of pixel-objects are shown by *circles*. Note locally noisy drifting of the pixel-objects. To aid understanding of the pixel-objects motion we labelled, in picture t=0, trajectories of three pixel-objects as $X1$ (start) and $X2$ (end), $X = A, B, C$. From [7]

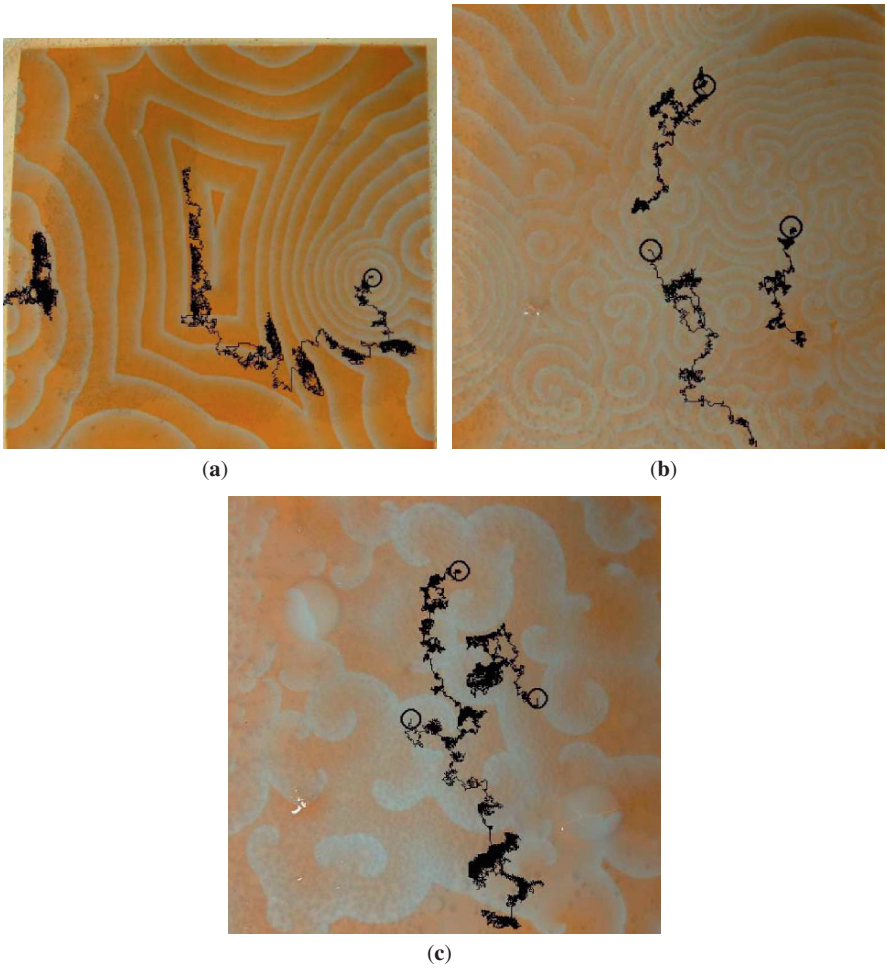

Fig. 11.11 Manipulation of pixel-sized objects in various regimes of excitation in BZ-medium. Initial positions of pixel-objects are shown by circles. Note locally noisy drifting of the pixel-objects in (**a**) and (**b**). (**a**) Example of influencing transportation by frequency of target-wave generation. Both pixel-objects were manipulated for 14,000 times steps. (**b**) Manipulating pixel-objects in a BZ medium with many sources of spiral waves. (**c**) Manipulating pixel-objects by wave-fragments in sub-excitable BZ medium. From [7]

waves. The objects accelerated by populations of spiral waves, can then be confined to a border-line domain between two sources of target waves or even slowed down by a single source of target-waves. A BZ medium in a sub-excitable mode, when localized wave-fragments inhabit the reactor space, may prove to be an invaluable tool for combining manipulation with logical decision making schemes. Each localized wave-fragment acts as a 'force bullet', which can be directed very precisely towards the manipulated object, and the force imparted to the object sends the manipulated shape in the desired direction.

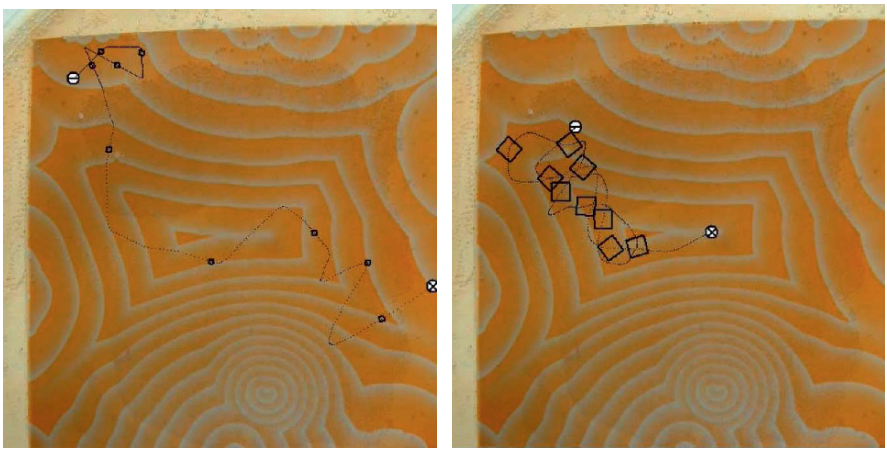

(**a**) (**b**)

Fig. 11.12 Snapshots of squares manipulated by the BZ medium during 500 steps. Trajectories of the centre of mass of the squares are shown by the *dotted line*. Exact orientation of theobjects is displayed every 50 steps. (**a**) square 5×5 cell size, (**b**) square 20×20 cell size. Initial position of object is shown by *circle with minus* and final position by *circle with x* . From [7]

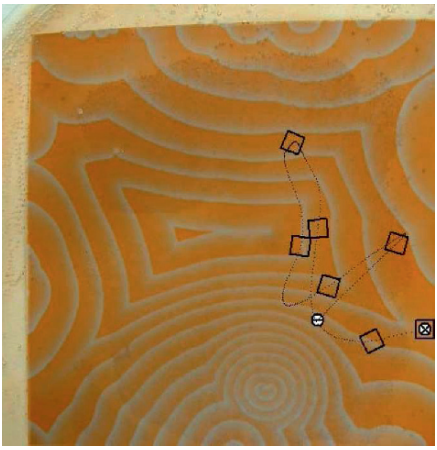

(**a**)

Fig. 11.13 (**a**) Snapshots of 20×20 cell square manipulated by BZ medium during 500 steps. Trajectory of centre of mass of the squares is shown by *dotted line*. Exact orientation of the object is displayed at every 50 steps. Initial position of the object is shown by *circle with minus* and the final position by *circle with plus*. From [7]

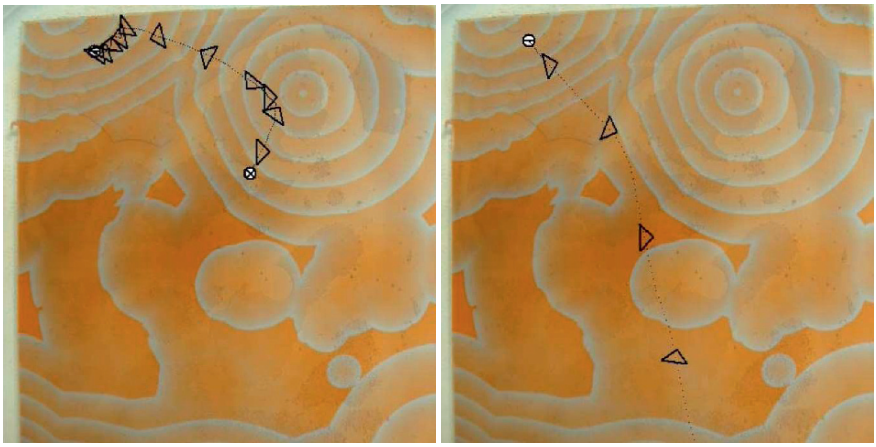

(**a**) (**b**)

Fig. 11.14 Snapshots of isosceles, right-angled triangle (size of half square) manipulated by BZ medium during 200 steps. Trajectories of the centre of mass of the triangle is shown by the *dotted line*. The exact orientation of the object is displayed at every 20 steps. Initial position of the object is shown by *circle with minus* and the final position by *circle with plus* . From [7]

11.5 Closed-Loop Control of Robotic Hand

In the previous sections, we described the design of chemical controllers for robots, which can calculate a shortest collision-free path in the robotic arena and guide the robot toward the source of stimulation (taxis). However, the controllers described a lack of feedback from the robot to the controller. In a set of remarkable experiments undertaken by Hiroshi Yokoi and Ben De Lacy Costello [4], it was demonstrated that when a closed-loop interface between the chemical controller and the robot is established, the behaviour of the hybrid systems becomes even more intriguing.

In experiments [4], the robotic hand developed in [9] was used. Each finger of the robotic hand consists of two pivots with springs and wire guides attached (Fig. 11.15a).

We use a spring coil type of stainless steel outer wire as a guide for nylon inner wire to realize the function of the spring. When a finger does not bend the spring coil type of outer wire keeps it straight. If a finger needs torque, the spring coil type of outer wire bends to realize the shortest route of the inner wire; the elastic wires are connected to servomotors (Fig. 11.15b). The motors are controlled by a microprocessor H8Tiny produced by Hitachi. The microprocessor has eight inputs from photo-sensors, and outputs linked to ten servomotors. The microprocessor encodes signals from sensors to run the motor drives. The finger motors are powered by 5 V, and the microprocessors are powered by 9 V. The hand is mounted above the chemical reactor and glass micro-pipettes filled with silver colloid solution were attached to the fingertips to stimulate the chemical medium (Fig. 11.16).

To enable the robotic hand to interact with the chemical processor, we attached glass capillary tubes filled with a solution of colloidal silver to the fingertips, and

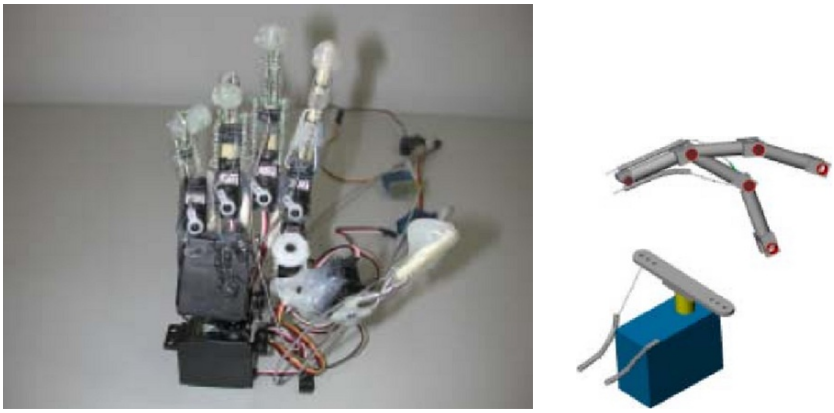

(**a**) (**b**)

Fig. 11.15 Hardware architecture of robotic hand. (**a**) Overall view of the hand. (**b**) Actuating fingers via elastic wires (*top*) by servomotor (*bottom*). From [4]

Fig. 11.16 Robotic hand interacts with Belousov–Zhabotinsky medium. From [4]

adjusted the hand above the Petri dish containing the BZ mixture in such a way that when a finger bent by a significant amount the pipettes were immersed just below the surface of the mixture releasing a defined quantity of silver and initiating additional excitation waves in the chemical medium.

To detect excitation wave fronts in the chemical reactor, we used photodiodes (VTB8440B), with a quoted spectral application ranging from 330 to 720 nm (Fig. 11.17). When a wave front travels through the medium and across the sensor, this is detected directly and the sensor's output current increases, this increase is detected by the micro-controller, which starts the servomotor causing the corresponding finger to bend. The fingers are programmed to straighten again a few seconds after bending.

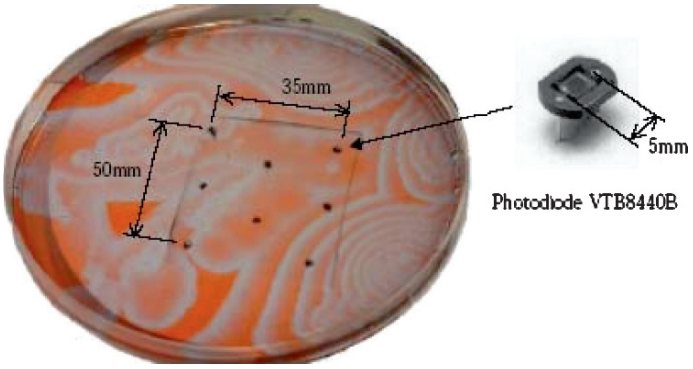

Fig. 11.17 Sensory system of the BZ-Hand. Experimental chemical reactor with photo-sensors underneath (*left*), sensors are visible as black sites on the photograph, and a view of the single sensor (*right*). From [4]

A typical development in the studied system is as follows: when one or more fingers bend for the first time (due to a solitary circular wave initiated at the reactors edge and moving towards the centre of the reactor – thus, crossing all photo-sensors), colloidal silver from the glass micro-pipettes, attached to the fingers, is deposited locally into the medium and initiates a series of excitation waves (Fig. 11.16).

A series of waves is initiated as silver colloid is physically deposited into the system and depending on the amount (proportional to the time the finger is in contact with the surface), it will usually initiate a number of waves at or near the contact point when the system has regained its excitability. As silver diffuses from the sites of contact, multiple excitation sites may be established leading to complex waves or spiral waves (also caused by the disturbance of the reactor surface by the motion of the fingers).

When the excitation waves spread, they stimulate photo-sensors, attached to the underneath of the Petri dish and this causes further bending of the fingers. Let us consider the behaviour of the system when up to three fingers have the ability to move.

The position of the sensors controlling these fingers and the sites where the fingers' touch the medium are shown in Fig. 11.18. When only one finger is operational, it excites (in the first instance) a generalized target wave in the medium. The wavefronts are detected by the sensor and the finger bends delivering more activator (silver) to the system and continuing the excitation process or disrupting existing waves. Thus the system enters a mode of self-excited oscillatory motion (Fig. 11.19a). If two fingers are operational and just one finger bends, then, after some transient period, the robotic hands fingers act in anti-phase because they reciprocally stimulate each other via the wavefronts of the target waves they initiate (Fig. 11.19b).

When both fingers touch the BZ medium at the beginning of the experiment the system starts to exhibit synchronous oscillations (11.19c). This happens because

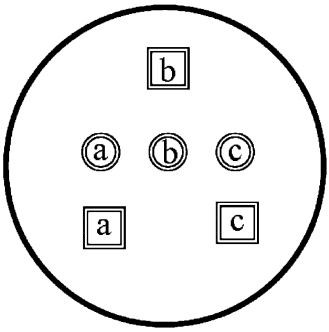

Fig. 11.18 Schematic relative positions (*circles*) of sensors affecting index (a), middle (b) and third (c) digits of the robotic hand, and sites (*rectangles*) where these fingers stimulate the BZ medium

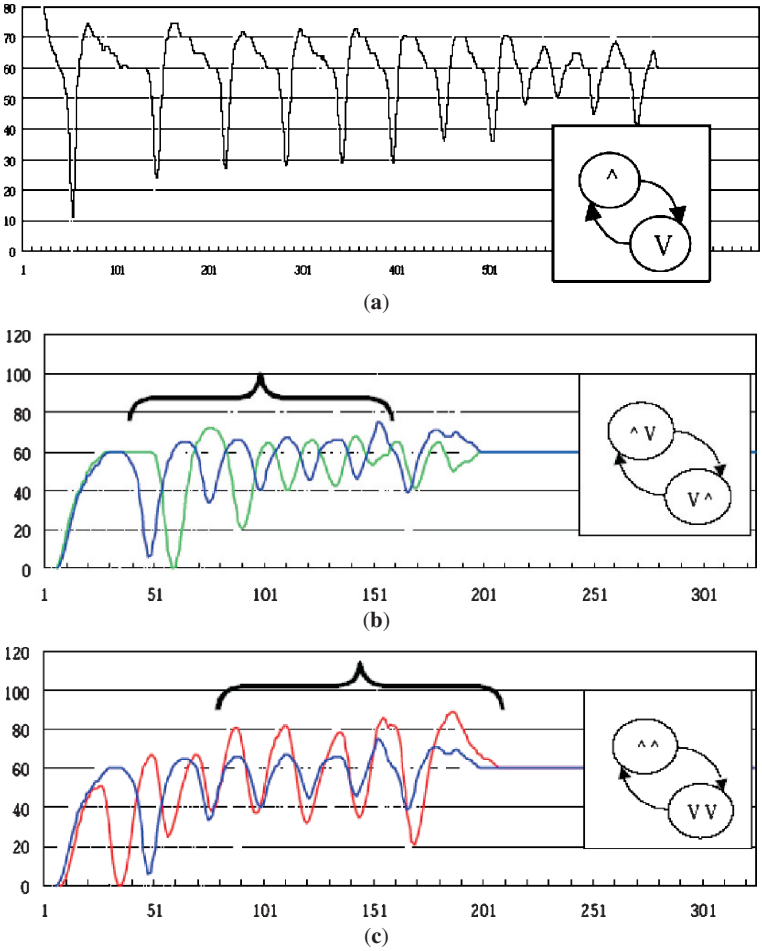

Fig. 11.19 Typical modes of "Fingers – BZ medium" system for one (**a**), and two (**b**) and (**c**), fingers. Voltage on the photo-sensor is shown in vertical axis; time in seconds is shown in horizontal axis. Corresponding movements of the finger are outlined in the insert, *U* means up and *D* down.

the wavefronts of the target waves, initiated by the movement of the fingers, cancel each other out when they collide, and thus, as in the general situation, each finger excites only itself. When three fingers are operated simultaneously, highly complex behaviors are observed (whatever the the starting configuration) – eventually, the system may appear to reach an almost synchronized or repetitive motion, but this is then subject to major transient fluctuations.

See [4] for details of complex dynamics of interactions between BZ medium and the robotic hand.

11.6 Physarum Robots

Plasmodium, the vegetative stage of the slime mould *Physarum polycephalum*, is a single cell, with thousands of diploid nuclei, formed when individual flagellated cells or amoebas swarm together and fuse. The plasmodium is visible with the naked eye. When plasmodium is placed on an appropriate substrate, the plasmodium propagates and searches for sources of nutrients (bacteria). When these sources are located and taken over, the plasmodium forms veins of protoplasm. The veins can branch, and eventually the plasmodium spans the sources of nutrients with a dynamic proximity graph, resembling, but not perfectly matching graphs from the family of k-skeletons [10].

The large size of the plasmodium allows the single cell to be highly amorphous. The plasmodium shows synchronous oscillation of cytoplasm throughout its cell body, and oscillatory patterns control the behaviour of the cell. All the parts of the cell behave cooperatively in exploring the space, searching for nutrients and optimizing a network of streaming protoplasm. Because of its unique features and the relative ease of undertaking laboratory experiments, the plasmodium became a test biological substrate for the implementation of various computational tasks.

The problems solved by the plasmodium include maze-solving [11–13], calculation of efficient networks [14] and proximity graphs [10], construction of logical gates [15] and robot control [16].

Can the plasmdoium be considered as a reaction–diffusion amorphous robot? Yes, as shown in more details in [17]. The oscillatory cytoplasm of the plasmodium can be seen as a spatially extended nonlinear excitable media [18–20]. In our previous papers, we hypothesized that the plasmodium of Physarum is a biological analogue of a chemical reaction–diffusion system, encapsulated in an elastic and growing membrane [17]. Such an encapsulation enables the plasmodium to function as a massively-parallel reaction–diffusion computer [3] and also to solve few tasks, which reaction–diffusion computers could not do, e.g. construction of spanning trees [21], and implementation of storage modification machines [22].

Being encapsulated in an elastic membrane, the plasmodium is capable of not only computing spatially distributed data-sets but also physically manipulating elements of the data-sets. If a sensible, controllable and programmable movement of the plasmodium could be achieved, this would open the way for experimental

implementation of amorphous robotic devices. There are already seeds of an emerging theory of artificial amoeboid robots [23–25].

We discuss a set of scoping experiments on establishing links between Physarum computing and Physarum robotics. We will show that plasmodium can in principle be used to manipulate lightweight objects in a controllable way according to the positioning of nutrients' sources and can, therefore, be considered an example of a living amoeboid robot. We chose the surface of water as a physical substrate for the development of the plasmodium because in this mode the plasmodium network can be dynamically updated without being stuck to a non-liquid substrate and therefore, small objects floating on the surface can be manipulated by the plasmodium's pseudopodia with ease.

Plasmodium of *Physarum polycephalum* was cultivated on wet paper towels in dark ventilated containers, oat flakes were supplied as a substrate for bacteria on which the plasmodium feeds. We used several test arenas for observing the behaviour of the plasmodium and scoping experiments on the plasmodium-induced manipulation of floating objects. These are Petri dishes with base diameters 20 and 90 mm, and rectangular plastic containers 200 by 150 mm. The dishes and containers were filled to 1/3 depth with distilled water. Data points, to be spanned by the plasmodium, were represented either by 5–10 mm sized pieces of plastic foam, which were either fixed to the bottom of the Petri dishes or left floating on the water surface. Oat flakes were then placed on top of the foam pieces. Foam pieces, where the plasmodium was initially placed, and the pieces with oat flakes were anchored to the bottom of containers. Tiny foam pieces to be manipulated by the plasmodium were left free-floating.

To demonstrate that a substrate is suitable for robotic implementation, one must demonstrate that the substrate is capable of sensing the environment coupled with responsiveness to external stimulus, it must be capable of solving complex computational tasks on spatially distributed data sets and demonstrate locomotion and/or manipulation of objects. We provide basic demonstrations, which may indicate that plasmodium of *Physarum polycephalum* can be successfully used in future experiments on laboratory implementations of amorphous biological robots.

The surface of water has a high surface tension and therefore, it is physically able to support propagating plasmodium, when its contact weight to contact area ratio is small. When placed in an experimental container, the plasmodium forms pseudopodia aimed at searching for sources of nutrients. In most experiments the 'growth part' of the pseudopodia adopts a tree-like structure to achieve fine detection of chemo-gradients in the medium. This also happens to minimize the weight to area ratio of the system. Examples of tree-like propagating pseudopodia are shown in Fig. 11.20ab.

In Fig. 11.20b, we can see that not always pseudopodia grow towards source of nutrients, there is a pseudopodia growing South–west, where no sources of nutrients located. This happens possibly because in large-sized containers volume of air is too large to support a reliable and stationary gradient of chemo-attractants. This may pose a difficulty for the plasmodium to locate and span all sources of nutrients in large-sized containers.

Fig. 11.20 The plasmodium explores the experimental arena by use of propagating tree-like pseudopodia. From [26]

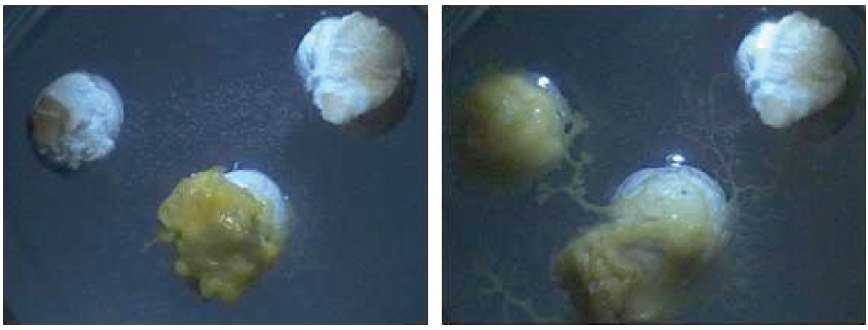

Fig. 11.21 Plasmodium builds links connecting its original domain of residence with two new sites. Initial position of plasmodium is in the photograph on the *left*, propagated plasmodium after 12 h is in the photograph on the *right*. From [26]

In Petri dishes the volume of air is small and, air is fairly static as it is an enclosed system. Therefore, the plasmodium easily locates the various sources of nutrients in its immediate vicinity (Fig. 11.21). Over the time it, therefore, constructs spanning trees where the graph nodes are represented by foam pieces containing oat flakes. In Fig. 11.21, we can see that originally the plasmodium was positioned at the Southern domain. In 12 h, the plasmodium builds a link with Western domain, and then starts to propagate pseudopodia toward the Eastern domain. When the plasmodium spans sources of nutrients, it produces many 'redundant' branches (Fig. 11.21). These branches of pseudopodia are necessary for space exploration but do not represent minimal edges connecting the nodes of the spanning tree. These 'redundant' branches are removed at a later stage of the spanning tree development. A well-established spanning tree of data-points is shown in Fig. 11.22. Initially, the plasmodium was placed in the Western domain, and the plasmodium constructed a spanning tree in 15 h.

We demonstrated that the plasmodium explores the domain space and computes a spanning tree across the surface of water, when placed initially on one of the floating objects. Would the plasmodium be successful if placed directly on the surface

of the water? As we can see in Fig. 11.4, the plasmodium works perfectly. We placed a piece of plasmodium on the surface of water (Fig. 11.4, start) and in 3 h the plasmodium forms an almost circular front of propagating pseudopodia, these reach two stationary domains containing nutrients in 8 h (Fig. 11.4).

In usual conditions (on a wet solid or gel substrate), edges of spanning trees presented by protoplasmic tubes, adhere to the surface of the substrate [14, 21, 22]. Therefore, the edges cannot move, and the only way the plasmodium can dynamically update is to make a protoplasmic tube inoperative and to form a new edge instead (membrane shell of the ceased link will remain on the substrate, e.g. see [22]. When plasmodium operates on water surface, cohesion between the water surface and membrane of protoplasmic tubes is small enough for the protoplasmic tubes to move freely. Thus, the plasmodium can make the tubes almost straight and minimize "costs" of the transfer and communication between its distant parts. Two examples of the straightening of the protoplasmic tubes are shown in Fig. 11.24. Such straightening is a result of the tubes becoming shorter due to contraction.

Presence of a contraction may indicate that if two floating objects (both with sources of nutrients) are connected by a protoplasmic tube, then the objects will be pulled together due to shortening of the protoplasmic tube. We did not manage to demonstrate this exact phenomenon of pulling two floating objects together; however, we got experimental evidence of pushing and pulling of single floating objects by the plasmodium's pseudopodia. The plasmodium-induced pushing and pulling are exemplified in Figs. 11.25 and 11.26.

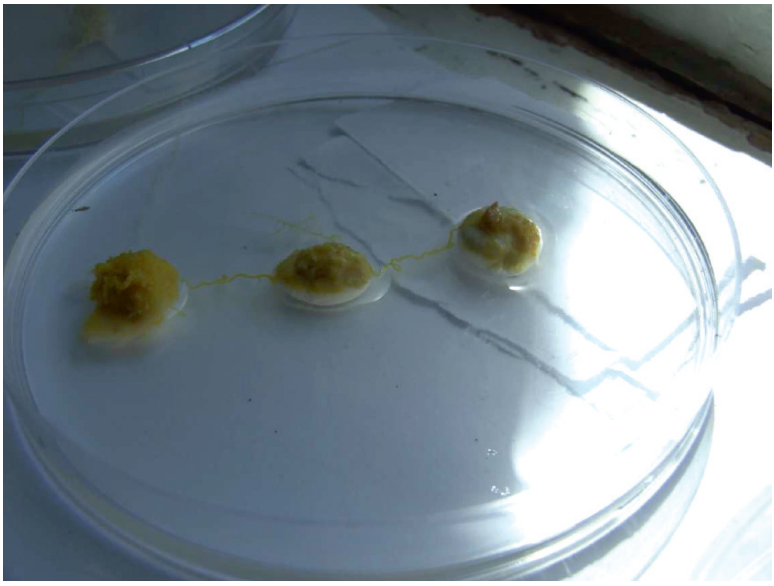

Fig. 11.22 Spanning tree of three points constructed by the plasmodium. From [26]

To demonstrate pushing, we placed a very lightweight piece of plastic foam on the water surface near the plasmodium (Fig. 11.25, 0 h). The plasmodium develops a pseudopodium, which propagates toward the lightweight piece of foam (Fig. 11.25, 5 h). Owing to gravitational force acting on the pseudopodia a ripple is formed on the water surface (Fig. 11.25, 9 h), which causes the piece of foam to be pushed away from the growing pseudopodia's tip (Fig. 11.25, 13 h). Due to the absence of any nutrients on the pushed piece of foam, the plasmodium abandons its attempt to occupy the piece and retracts the pseudopodia (Fig. 11.25, 16 h). The piece remains stationary: but is shifted away from its original position.

In the second example, Fig. 11.26, we observe pulling of the lightweight object. The piece of foam to be pulled is placed between two anchored objects (Fig. 11.26, 0 h). One object hosts the plasmodium and other object has an oat flake on top (i.e. attracts the plasmodium). A pseudopodium grows from the plasmodium's original location toward the site with the source of nutrients. The pseudopodium occupies this piece of foam (Fig. 11.26, 15 h) and then continues its propagation toward the source of nutrients. When the source of nutrients is reached (Fig. 11.26, 22 h) the protoplasmic tubes connecting the two anchored objects contract and straighten, thus, causing the lightweight object to be pulled toward the source of nutrients (Fig. 11.26, 32 h). The pushing and pulling capabilities of the plasmodium can be utilized in construction of water-surface based distributed manipulators [7, 8, 27].

Fig. 11.23 Plasmodium starts its development on the water surface and occupies two sources of nutrients. (**a**) initial position of the plasmodium, (**b**) 3 h, (**c**) 5 h, (**d**) 8 h. From [26]

11.7 Conclusion

In examples of chemical based laboratory prototypes, we demonstrated that chemical reaction–diffusion media are promising, non-silicon distributed controllers for robotics. They are capable of controlling the robot motion in response to external stimulation. They efficiently act as underlying parallel architectures for distributed and intelligent robotic manipulators, which can be integrated into a closed-loop robotic system. Moreover, when encapsulated in an elastic membrane, the reaction–diffusion systems provide an optimal platform for amorphous embedded intelligence.

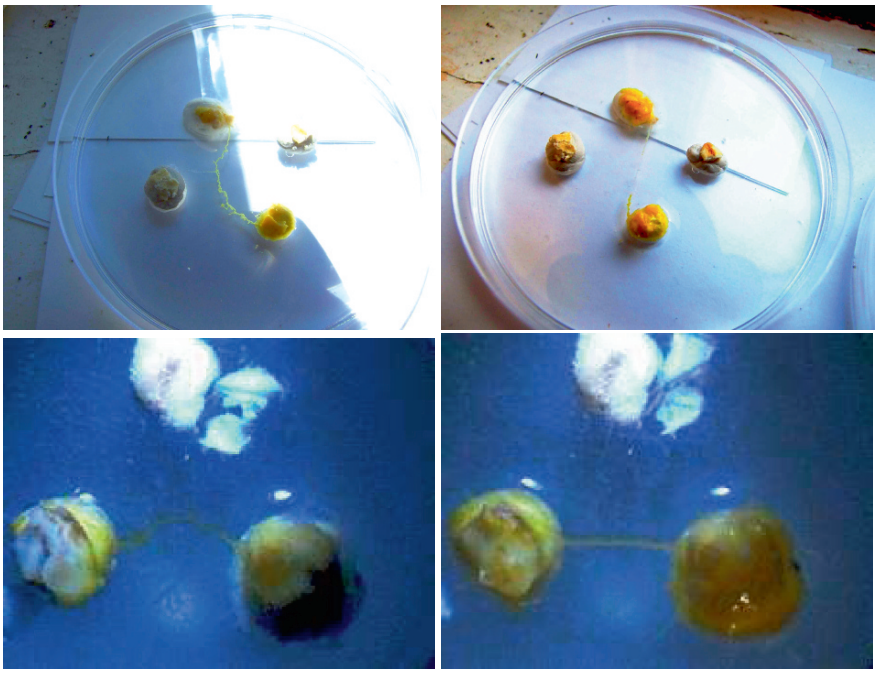

Fig. 11.24 Examples of straightening of protoplasmic tubes. In photographs (**a**) and (**c**) tubes are longer than necessary. In photographs (**b**) and (**d**) the tubes correspond to minimal shortest path between the sites they are connecting. Time interval between the recordings (**a**) and (**b**), and (**c**) and (**d**) is 12 h. From [26]

In experimental conditions, we have shown that it is indeed possible to guide a mobile robot with an onboard excitable chemical processor. To stimulate the robot, and to implement its taxis, we locally perturb concentrations of chemical species in the reactor. Excitation wave fronts propagating in the reactor carry (in their asymmetric wavefronts) information about original position of the stimulation source. Therefore, from images of spatio-temporal dynamics of excitation in the chemical

reactor, the robot extracts a direction toward the source of stimulation and implements rotation and forward motion.

We experimentally demonstrated a non-trivial concurrent interaction between an excitable chemical medium and a robotic sensing and actuating device. We proved that it is indeed possible to achieve some sensible control of a robotic hand using travelling and interacting excitation wave fronts in a liquid-phase BZ system. We discovered several patterns of finger movements: self-excited motion, synchronized motion of fingers and reciprocal motion of fingers. To demonstrate viability of the approach, we studied a closed-loop system where the robotic hand excites wave dynamics and these dynamics cause further movement of the hand's fingers.

We presented results of scoping experiments on manipulating simple objects in a simulated massive-parallel array of actuators controlled by experimental excitation dynamics in a BZ based chemical medium. Our basic assumption was that manipulated objects should be pushed by travelling excitation wavefronts. Therefore, we encoded snapshots of gel-based BZ media and converted them into arrays of local force vectors in such a manner that every pixel of the medium's snapshot got its own force vector, the orientation of which was determined by the gradient of the red component (which in turn represents concentrations of chemical species in the medium) in the neighbourhood of the pixel. Thus, e.g. a circular wave in the BZ medium – via the simulated actuator array – transports a manipulated object centrifugally, outward from the the wave's source of origin.

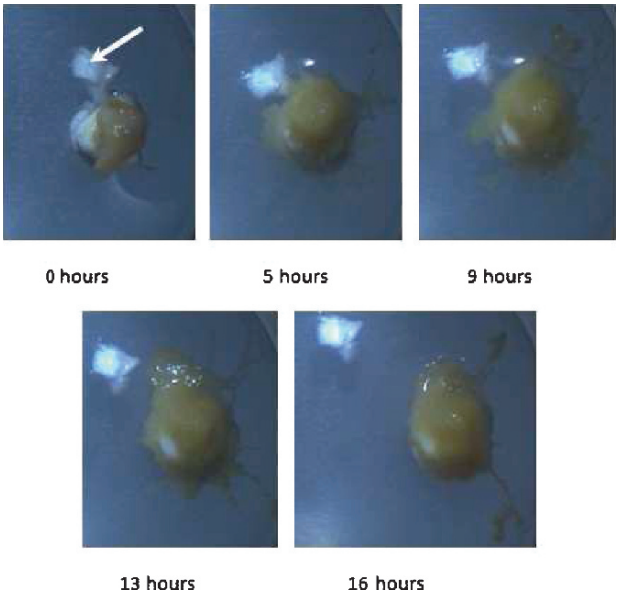

Fig. 11.25 Photographs demonstrate that the plasmodium can push lightweight floating objects. The object to be pushed is indicated by a *white arrow* in the first photograph of the series. From [26]

We also demonstrated that various types of excitation dynamics – target waves, spiral waves, wave-fragments – are capable of the transportation and manipulation of small objects (the size of which is comparable to an elementary micro-volume of the medium) and larger, spatially extended objects, planar shapes. Results on manipulation of spatially extended objects may find practical implementation in developing soft-robots and gel-based actuating surfaces. This may possibly lead to a hybrid amoeba-like robot capable of implementing flexible movement strategies and also grasping and manipulating objects in the environment.

The integration of chemical controllers to hardware components has its drawbacks. Namely, chemical processors are not efficient when integrated in conventional hardware architectures. Any standard wheeled-robot with primitive

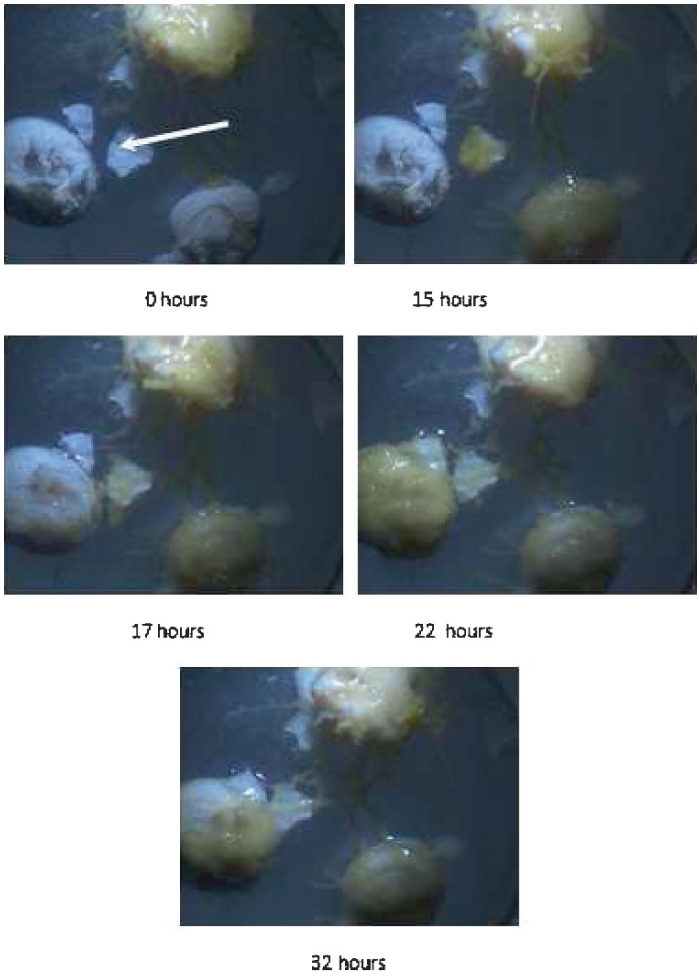

Fig. 11.26 Photographs demonstrate that the plasmodium can pull lightweight objects. The object to be pulled is indicated by white arrow in the first photograph. From [26]

photo-sensors will outperform a chemical-medium-controlled robot in any navigation task. Not only the reaction–diffusion algorithms, when implemented in a chemical medium are slow, but also the analysis of the medium space–time dynamics consumes more computational resources compared to any simple program that can guide a standard mobile robot. However, wave-based control in disordered media will ideally suit amorphous robotic architectures, like those based on electro-activated and oscillating polymers.

The last thesis was proved in our experiments with the plasmodium of *Physarum polycephalum*. Inspired by bio-mechanics of surface walking insects, see e.g. [28–31], our previous studies on implementation of computing tasks in the plasmodium [17, 21, 22, 32] and our ideas on design and fabrication of biological amorphous robots [33], we explored the operational capabilities of the plasmodium of *Physarum polycephalum* on the surface of water. We showed that the plasmodium possesses the essential features of distributed robotics devices: sensing, computing, locomotion and manipulation.

We demonstrated experimentally that the plasmodium (1) senses data-objects represented by sources of nutrients, (2) calculates shortest path between the data-objects, and approximates spanning trees where the data-objects are nodes (in principle, a spanning tree of slowly moving data-objects can be calculated as well), (3) pushes and pulls lightweight objects placed on the water surface. The findings indicated that the plasmodium is a prospective candidate for the role of spatially extended robots implemented on biological substrates.

References

1. Zaikin, A.N., Zhabotinsky, A.M.: Concentration wave propagation in two-dimensional liquid-phase self-oscillating system. Nature 225, 535 (1970)
2. Adamatzky, A.: Computing in Automata Media and Automata Collectives. IoP (2001)
3. Adamatzky, A., De Lacy Costello, B., Asai, T.: Reaction Diffusion Computers. Elsevier (2005)
4. Yokoi, H., Adamatzky, A., De Lacy Costello, B., Melhuish C.: Excitable chemical medium controlled by a robotic hand: closed loop experiments. Int. J. Bifurcat. Chaos 14, 3347–3354 (2004)
5. Field, R. J., Winfree, A. T.: Travelling waves of chemical activity in the Zaikin–Zhabotinsky–Winfree reagent. J. Chem. Educ. 56, 754 (1979)
6. Adamatzky, A., De Lacy Costello, B., Melhuish, C., Ratcliffe, N.: Experimental implementation of mobile robot taxis with onboard Belousov–Zhabotinsky chemical medium. Mater. Sci. Eng. C 24, 541–548 (2004)
7. Adamatzky, A., De Lacy Costello, B., Skachek, S., Melhuish, C.: Manipulating objects with chemical waves: Open loop case of experimental Belousiv-Zhabotinsky medium. Phys. Lett. A, 350(3-4), 201–209, 6 February (2006)
8. Skachek, S., Adamatzky, A., Melhuish, C.: Manipulating objects by discrete excitable media coupled with contact-less actuator array: Open-loop case. Chaos Solitons Fractals 26, 1377–1389 (2005)
9. Ishikawa, Y., Yu, W., Yokoi, H., Kakazu, Y.: Development of robot hands with an adjustable power transmitting mechanism, In: Cihan H. Dagli et al. Eds. Proc. Intell. Engineer. Syst. Through Artificial Neural Networks 10, 631–636 (2000)
10. Adamatzky, A.: Does Physarum follow Toussaint conjecture? Parallel Processing Letters (2008)

11. Nakagaki, T., Yamada, H., Toth, A.: Maze-solving by an amoeboid organism. Nature 407, 470–470 (2000)
12. Nakagaki T.: Smart behavior of true slime mold in a labyrinth. Res. Microbiol. 152, 767–770 (2001)
13. Nakagaki T., Yamada H., Toth A.: Path finding by tube morphogenesis in an amoeboid organism. Biophys. Chem. 92, 47–52 (2001)
14. Nakagaki, T., Yamada, H., Hara, M.: Smart network solutions in an amoeboid organism. Biophys. Chem. 107, 1–5 (2003)
15. Tsuda, S., Aono, M., Gunji, Y.-P.: Robust and emergent Physarum computing. BioSystems 73, 45–55 (2004)
16. Tsuda, S., Zauner, K. P., Gunji, Y. P.: Robot control with biological cells. Biosystems, 87, 215–223 (2007)
17. Adamatzky, A.: Physarum machines: encapsulating reaction-diffusion to compute spanning tree. Naturwisseschaften (2007)
18. Matsumoto, K., Ueda, T., Kobatake, Y.: Reversal of thermotaxis with oscillatory stimulation in the plasmodium of Physarum polycephalum. J. Theor. Biol. 131, 175–182 (1998)
19. Nakagaki, T., Yamada, H., Ito, M.: Reaction-diffusion-advection model for pattern formation of rhythmic contraction in a giant amoeboid cell of the Physarum plasmodium J. Theor. Biol. 197, 497–506 (1999)
20. Yamada H., Nakagaki T., Baker R. E., Maini P.K.: Dispersion relation in oscillatory reaction-diffusion systems with self-consistent flow in true slime mold. J. Math. Biol. 54, 745–760 (2007)
21. Adamatzky A. Growing spanning trees in plasmodium machines. Kybernetes, 37, 258–264 (2008)
22. Adamatzky, A.: Physarum machine: implementation of a Kolmogorov-Uspensky machine on a biological substrate. Parallel Process. Lett. 17 (2008)
23. Shimizu, M., Ishiguro, A.: Amoeboid locomotion having high fluidity by a modular robot. Int. J. Unconventional Comput. (2008), in press
24. Yokoi, H., Kakazu, Y.: Theories and applications of autonomic machines based on the vibrating potential method, In: Proc. Int. Symp. Distributed Autonomous Robotics Systems, 31–38 (1992)
25. Yokoi, H., Nagai, T., Ishida, T., Fujii, M., Iida, T.: Amoeba-like robots in the perspective of control Architecture and morphology/materials, In: Hara, F. and Pfeifer, R. (Eds.) Morpho-Functional Machines: The New Species, Springer, Tokyo, 99–129 (2003)
26. Adamatzky, A.: Towards Physarum robots: computing and manipulating on water surface (2008) arXiv:0804.2036v1 [cs.RO]
27. Hosokawa, K., Shimoyama, I., Miura, H.: Two-dimensional micro-self-assembly using the surface tension of water. Sens. Actuators A 57, 117–125 (1996)
28. McAlister, W. H.: The diving and surface-walking behaviour of Dolomedes triton sexpunctatus (Araneida: Pisauridae). Animal Behav. 8, 109–111 (1959)
29. Suter, R. B., Wildman, H.: Locomotion on the water surface: hydrodynamic constraints on rowing velocity require a gait change. J. Exp. Biol. 202, 2771–2785 (1999)
30. Suter, R. B.: Cheap transport for fishing spiders: the physics of sailing on the water surface. J. Arachnol. 27, 489–496 (1999)
31. Suter, R. B., Rosenberg, O., Loeb, S., Wildman, H., Long, J. Jr.: Locomotion on the water surface: propulsive mechanisms of the fisher spider, Dolomedes triton. J. Exp. Biol. 200, 2523–2538 (1997)
32. Adamatzky, A., De Lacy Costello, B., Shirakawa T.: Universal computation with limited resources: Belousov-Zhabotinsky and Physarum computers. Int. J. of Bifurcation and Chaos (IJBC), 18(8), 2373–2389 (2008)
33. Kennedy, B., Melhuish, C., Adamatzky, A.: Biologically Inspired Robots in In: Y. Bar-Cohen (Ed) Electroactive polymer (EAP) actuators – Reality, Potential and challenges. SPIE, (2001)